Magnetism in Solids

Effect of oblique versus normal deposition orientation on the properties of perpendicularly magnetized $L1_0$ FePd thin films

Xinjun Wang,[1,2] Sergiy Krylyuk,[1] Daniel Josell,[1] Delin Zhang,[2] Jian-Ping Wang,[2,*] and Daniel B. Gopman[1,**]

[1]Materials Science and Engineering Division, National Institute of Standards and Technology, Gaithersburg, MD, 20899, USA
[2] Department of Electrical Engineering, University of Minnesota, Minneapolis, MN 55455 USA

* Fellow, IEEE
** Member, IEEE

Abstract— Materials such as $L1_0$ Fe-based alloys with perpendicular magnetic anisotropy derived from crystal structure have the potential to deliver higher thermal stability of magnetic memory elements compared to materials whose anisotropy is derived from surfaces and interfaces. A number of processing parameters enable control of the quality and texture of $L1_0$ FePd among them, including substrate, deposition temperature, pressure and seed and buffer layer. The angle of inclination between the substrate and the sputtering target can also impact the texture of $L1_0$ crystallization of sputtered Fe-Pd and magnetic properties of the derived thin films. This study examines the difference between FePd layers that have been magnetron sputter deposited on Cr(15 nm)/Pt, Ir, or Ru(4 nm)/FePd (8 nm)/Ru(2 nm)/Ta(3 nm) substrate layers at an oblique angle (30° tilt from the sputtering target) versus normal incidence (target facing the substrate). X-ray diffraction, ferromagnetic resonance spectroscopy and vibrating sample magnetometry were used to compare the degree of $L1_0$ order and static and dynamic properties of films deposited under both conditions. The films grown using the oblique orientation exhibit a stronger degree of $L1_0$ orientation, a larger magnetic anisotropy energy and a lower Gilbert damping, on all three buffer layers.

Index Terms—Magnetism in Solids, perpendicular magnetic anisotropy; MRAM; FePd; Gilbert damping

1. INTRODUCTION

Materials with large perpendicular magnetic anisotropy (PMA) are critical to realizing high-density and low-energy spintronic devices and logic devices that require high thermal stability and scalability [Mangin 2006, Meng 2006, Kent 2015]. In order to scale down the lateral size to near 10 nm junction areas, large magnetic anisotropy energy densities K_u and small Gilbert damping constant α values are required to maintain 10-year thermal stability and reasonably low power switching. The relatively low K_u and high α [Ikeda 2010] of well-known interfacial PMA materials such as Ta/CoFeB/MgO are problematic for next-generation spin memory and logic devices with 10-nm lateral scaling and sub-0.01 Gilbert damping.[Xu 2002, Krounbi 2015, Bhatti 2017]

$L1_0$ FePd thin films with large magnetocrystalline anisotropy ($\approx$ MJ/m^3) and low Gilbert damping (<.01) are attracting considerable interest for device applications. Its properties make FePd films of interest for electric-field control of magnetism [Weisheit 2007, He 2013], magnetostrictive transducers [Saito 2013, Yang 2013, Yang 2014], ultrahigh density granular storage media [Tokuoka 2014, Liu 2017], and spintronics [Lee 2014, Naganuma 2015, Hsu 2018, Xu 2018, Zhang 2018b]. It has been shown that high-quality FePd films with properties relevant for particular applications can be achieved through tuning of the growth process, including the substrate, substrate rotation, deposition temperature, seed/buffer layers, and deposition pressure [Chang 2015, Ohtake 2015, Futamoto 2016b, Futamoto 2016a, Zhang 2018b].

The angle of inclination between substrate and sputtering target can also impact $L1_0$ crystallization in sputtered FePd films. Among several noteworthy examples, oblique angle deposition has been used to engineer local structure at the nanoscale in Ti thin films[Alvarez 2016] as well as the phase of TiO_2 films for solar cell applications [Vrakatseli 2018]. It has also been used to control magnetic properties, including the anomalous magnetoresistance in thin permalloy films [Ali 2019], ordering in a CoCrPt alloy [Zheng 2002] and symmetry breaking in synthetic antiferromagnets coupled through an obliquely sputtered Ir spacer [Fernández-Pacheco 2019].

This work investigates the impact of a 30° inclination of the substrate relative to the sputtering target in realizing $L1_0$-ordered FePd films with (001)-orientation normal to the film plane. FePd thin films for spintronic applications are likely to require metallic buffer layers, either for crystallographic texturing or to deliver a spin polarized current in the case of spin-orbit-torque devices. This study seeks to determine whether a 30° inclination of the substrate relative to the sputtering target can maintain or improve an (001) growth direction on buffer layers (Ir, Pt and Ru) that are used in conventional CoFeB- or Co-based spintronic devices, and whether the substrate inclination can improve the degree of $L1_0$ ordering and the associated

Corresponding author: Daniel B. Gopman (daniel.gopman@nist.gov).
Digital Object Identifier: 10.1109/LMAG.XXXX.XXXXXXX (inserted by IEEE).

static and dynamic properties of FePd.

This investigation is constrained to Cr-seeded, MgO(001) single-crystalline substrates with three different buffer layers: Pt, which has been studied extensively for (001)-textured FePd [Caro 1997], Ru, which has recently been shown to crystallize in the metastable fcc (001) orientation in (001)-oriented FePd/Ru/FePd synthetic antiferromagnets [Zhang 2018a] and Ir, which has a notably good lattice match to FePd and is a potentially advantageous buffer layer for (001)-oriented FePd films. While x-ray diffraction indicates generally strong (001) texturing of the Cr/buffer/FePd films, exhibiting cube-on-cube growth on the MgO(001) substrates, the films grown using the oblique deposition exhibit a stronger degree of $L1_0$ ordering and a larger perpendicular magnetic anisotropy field. The microstructure resulting from oblique deposition yields better structural, and consequently magnetic, ordering for the films across all three buffer layer materials.

2. EXPERIMENTAL

Single-crystalline MgO (001) substrates were sonicated in acetone for 20 min, then boiled in isopropanol 20 min before insertion in vacuum. The substrates were subsequently heated at 60° per minute to 500 ºC (at pressure < 7×10^{-7} Pa) at which temperature they were held for one hour to further prepare the MgO surface for deposition.[Ohtake 2011, Futamoto 2016b] . The temperature was reduced to 350 ºC for film growth using direct current magnetron sputtering in a 0.4 Pa Argon environment under a 30 standard cubic centimeter per minute flow of ultrahigh purity Ar (99.999%) passed additionally through an in-line filter. Normal and oblique orientations of the substrate relative to the sputtering target were achieved by tilting the heated substrate stage relative to the FePd sputtering target; the substrate was tilted to either directly face the FePd sputtering target or 30° degrees away from it In both cases the distance from the FePd target to the center of the substrate stage is 17 cm, and azimuthal rotation of the substrate stage at approximately 2 rad/s was imposed to enhance deposition homogeneity. The sputtering targets were each 38 mm diameter and driven by 80 W direct current power, except for the FePd target, which was driven at 60 W. The samples used in this study had the following structure (thicknesses in parenthesis in nm): Cr(15)/BL(4)/FePd(8)/Ru(2)/Ta(3), where BL corresponds to the buffer layer, chosen as Pt, Ir or Ru. Deposition rates (in nm/min) for Cr (1.15), Pt (2.43), Ir (1.90), Ru (1.27), FePd (2.22 normal; 1.38 oblique based on projected area), and Ta (0.86) were estimated by x-ray reflectivity of calibration samples and confirmed with *in situ* quartz crystal thickness monitoring. A cylindrical metal chimney of 5 cm radius and 5 cm length was mounted to each of the sputtering sources, providing some collimation of the ballistic fluxes of material as well as prevent cross-contamination of the sources.

3. RESULTS AND DISCUSSION

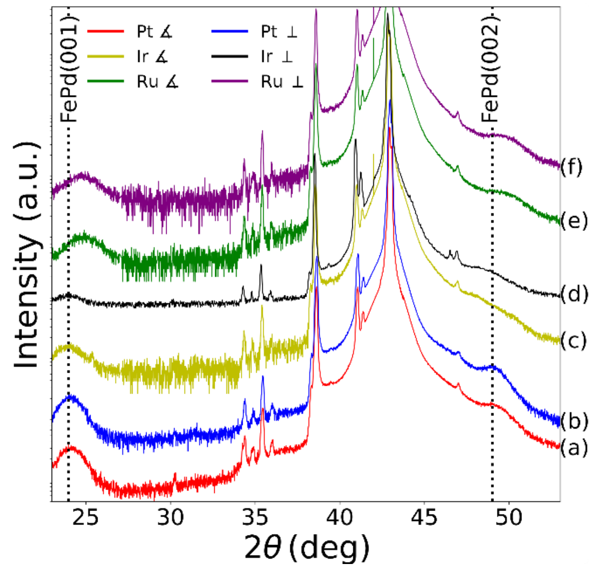

Figure 1. X-ray diffraction: comparing samples grown under normal or oblique deposition conditions for three different buffer layer combinations: (a) Pt oblique; (b) Pt normal; (c) Ir oblique; (d) Ir normal; (e) Ru oblique and (f) Ru normal.

Symmetric theta/two-theta x-ray diffraction scans were acquired on each specimen using a 9 kW rotating anode Cu-Kα x-ray source (0.15406 nm) and parallel beam optics. Intensity versus two theta scans of the FePd films using different substrate orientations for each of the three buffer layers are shown in Figure 1 with the bulk FePd (001) and (002) peak positions (c = 0.3715 nm) indicated for reference.[Futamoto 2016b] Diffraction peaks corresponding to the (002) lattice planes of $L1_0$ FePd are observed with every specimen, indicating a strong (001) texture and at least partial crystallization of the FePd alloy into the $L1_0$ phase regardless of buffer layer and angle of incidence for the FePd deposition. The lattice constant c of the $L1_0$ FePd thin films was evaluated from the (002) peak position. The degree of $L1_0$ ordering, S, was evaluated from the square root of the ratio of integrated intensities of the (001) and (002) FePd peaks $(I^{001}/I^{002})_{exp}$ estimated from Fig. 1, normalized by the theoretical intensity ratio $(I^{001}/I^{002})_{th}$, whose value (0.73) is estimated from the intrinsic scattering factors and extrinsic factors relevant to the x-ray diffractometer.[Yang 2012] The lattice constant c and order parameter S are summarized in Table I. The FePd (001) and (002) peaks are shifted to higher angles for the Ru-buffered films for both oblique and normal inclination, which may be an indication of interdiffusion between the buffer layer and the FePd film, which is also supported by x-ray reflectivity measurements of the normal inclination Ru-buffered film, where our best model to the data includes a diffuse Ru/FePd interface. As can be seen from the Table, within one sigma uncertainty, there is no apparent influence of the substrate inclination on the out-of-plane lattice constant of FePd for a given buffer layer composition. On the other hand, the order parameter of the specimens with obliquely deposited FePd are systematically higher than those grown under normal deposition conditions.

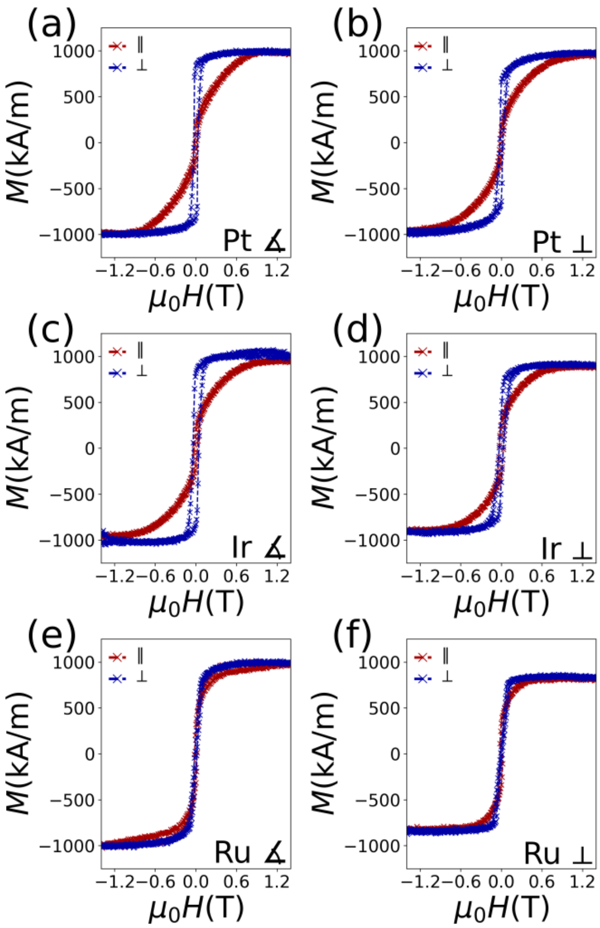

Figure 2: Magnetization versus applied external field for both out-of-plane and in-plane applied magnetic fields, for films with the three barrier layers and FePd films deposited using oblique and normal orientations: (a) Pt oblique; (b) Pt normal; (c) Ir oblique; (d) Ir normal; (e) Ru oblique and (f) Ru normal.

Magnetization versus applied external field hysteresis loops under in-plane and perpendicular field orientations were measured using a vibrating sample magnetometer. Compared with normal FePd deposition, films produced by oblique deposition systematically exhibit a larger saturation field in-plane (see Figs. 2(a)-2(b)), indicative of a larger perpendicular anisotropy field (H_k). Moreover, the oblique films exhibited a relatively higher out-of-plane coercive field (H_c), and larger magnetic remanence (M_r), consistent with a stronger preference for perpendicular magnetization in those samples. The saturation magnetization (M_s) for the samples is summarized in Table 1. Samples deposited under normal deposition exhibited lower saturation magnetization values than those grown under an oblique angle, particularly within the Ru series, which could be consistent with intermixing or diffusion at the interface with the buffer layer.

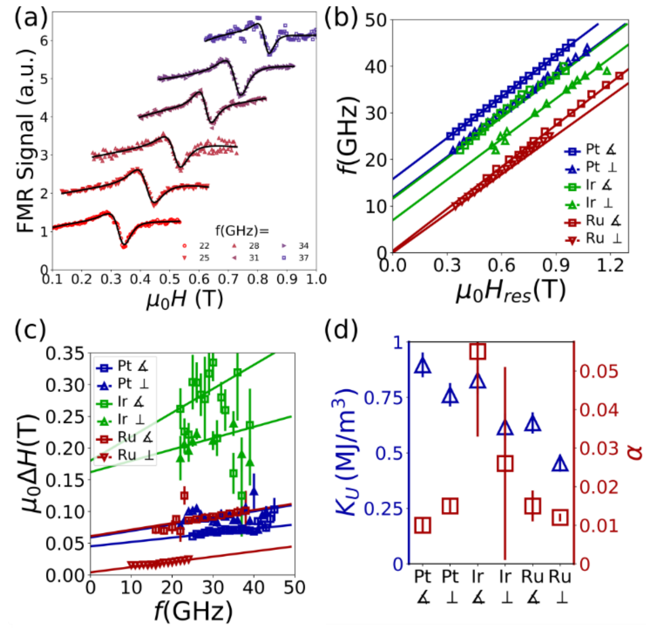

Figure 3. Ferromagnetic resonance results, including: (a) representative absorption curves for the Pt buffered sample with FePd deposited under normal orientation; (b) frequency versus resonance field spectra; (c) linewidth versus frequency and (d) K_U and α summary.

Ferromagnetic resonance (FMR) measurements were taken to deliver a more quantitative estimate of the perpendicular magnetic anisotropy field as well as the Gilbert damping in the films. Samples were placed film side down on a two-terminal, grounded coplanar waveguide (GCPWG) oriented between the poles of an electromagnet with the generated field applied perpendicular to the film plane. A radio frequency current was injected at one terminal and the transmitted power was detected from a diode detector at the second terminal. Helmholtz coils added an alternating field at 377 Hz, 1 mT peak amplitude, to enable lock-in detection of the differential ferromagnetic resonance absorption signal measured from the detector. For each sample, absorption was measured as a function of applied out-of-plane magnetic field over a range of frequencies to ascertain both the ferromagnetic resonance field versus frequency spectrum and the linewidth versus frequency spectrum. Figure 3(a) shows representative absorption curves for the Cr/Pt buffered sample deposited at normal incidence at six different frequencies. The lineshapes shown in Fig. 3(a) are each fit with the derivative of a Lorentzian lineshape, from which the resonance field (H_{res}, the zero-crossing) and linewidth (ΔH, the full-width at half maximum of the integrated intensity) The ferromagnetic resonance relationship between microwave excitation frequency and resonant applied magnetic field for fields applied normal to the thin film plane and linewidth versus frequency dispersion are given by [Farle 1997, Kaidatzis 2019]:

$$\left(\frac{f}{\gamma}\right)_{\perp} = \mu_0 H_{\mathrm{res}} + \mu_0 H_{\mathrm{eff}}^{\perp} \quad (1) \text{ and}$$

$$\mu_0 \Delta H = \frac{2\alpha}{\gamma} f + \mu_0 \Delta H_0, \quad (2)$$

H_{res} is the resonance field, $\gamma = g\mu_B/\underline{h}$ is the gyromagnetic ratio, g is the spectroscopic g-factor, μ_B is the Bohr magneton, h is the Planck constant, μ_0 is the vacuum permeability, $\mu_0 H_{\mathrm{eff}}^{\perp} = \mu_0 H_K - \mu_0 M_s$ is the effective perpendicular anisotropy field, α is the Gilbert damping parameter and ΔH_0 is the inhomogeneous linewidth broadening. Figure 3(b) displays the relationship between frequency and ferromagnetic resonance field for the three buffer layers under normal and oblique deposition conditions. Error bars in Figs. 3(b)-3(c) reflect the one-sigma uncertainty in fitting the resonance lineshape and applied field uncertainty, while uncertainty in Fig. 3(d) also includes uncertainty from estimation of the saturation magnetization shown in Table 1. The superimposed lines on Fig. 3(b) reflect the best linear fit to the Kittel relation from Eq. (1). Figure 3(d) summarizes the estimated magnetic anisotropy ($K_u = \mu_0 H_K / 2M_s$) for the buffer layers and the two deposition methods. Where the largest anisotropy energy from the obliquely deposited FePd on Pt buffer (0.90 MJ/m^3), we see the lowest anisotropy energy on the normal deposited FePd on Ru buffer (0.45 MJ/m^3). Consistent across the buffer layers, the sample deposited using normal deposition had lower anisotropy energies than their obliquely deposited counterparts.

From the best-fit lines to our linewidth versus frequency data (Fig. 3 (c)), we extract the Gilbert damping factor α for each buffer layer and deposition orientation, shown in Fig. 3(d). The lowest Gilbert damping value was observed in the Cr/Pt oblique sample (0.010(2)), which is consistent with also showing the largest anisotropy energy and highest order parameter (0.71) in the series. As can be seen in both Ir-buffered samples, significantly large line broadening was evident, indicative of the significance of buffer layer composition on the linewidth through spin pumping and inhomogeneous line broadening. While FePd typically exhibits a reduction in Gilbert damping with increases in ordering, the Ru series unexpectedly showed a lower damping for the less-ordered, lower S film grown with the normal orientation. Considering the diminished lattice parameter for the Ru series and the low saturation magnetization, we may anticipate that intermixing at the Ru/FePd interface during normal deposition could be producing a Fe-Pd-Ru composition with lower damping. The overall parameters are summarized in Table I.

Clearly, the substrate orientation during deposition plays a significant role in the $L1_0$ ordering, and thereby the static and dynamic properties of sputtered FePd films. The substrate orientation directly determined the deposition rate, which thereby enables or inhibits surface diffusion and atom relocation. The melting point of bulk FePd is T_M = 1310 ºC, so with a process temperature of 350 ºC, the film is equilibrating in an environment around 0.27 T_M, approximating the Thornton Zone Model Zone T, where surface diffusion is particularly relevant during growth, and changing the incident flux can play a large role in determining the kinetics of ordering, as in this temperature range grain boundaries and dislocations are mobile, so that recrystallization and grain growth become important to crystal growth [Ikeda 2010]. For oblique deposition, the deposition rate is reduced, which gives additional time for a given adatom to diffuse into minimum energy sites to facilitate $L1_0$ crystallization prior to the arrival of subsequent layers. Indeed, one previous study on $L1_0$ ordering of FePt films grown on Cr-buffered glass indicated a strong inverse proportionality between deposition rate and order parameter [Sun 2010]. On the other hand, the FePd films presented here were heteroepitaxially grown on single-crystalline MgO(001) with a Cr(001) seed layer and a (001) Pt(Ru,Ir) buffer layer, and may not be as sensitive to deposition rate due to the better lattice match to the underlying layer. Indeed, the FePt study found that the order parameter was vanishingly small at the deposition rates used in this study (1.4 nm/min and 2.2 nm/min, respectively for oblique and normal substrate inclination), while the FePd films shown herein have a comparatively large degree of $L1_0$ order.

We conjecture instead that the momentum of arriving atoms plays the leading role in this process. While a lower deposition rate provides more time for arriving adatoms to diffuse into ordered $L1_0$ sites, the role of tilting the substrate 30 degrees not only delivers additional transverse momentum to the arriving adatom to diffuse on the surface, but reduces the arriving momentum transferred by the kinetic arriving adatom (typically around 5 – 10 eV), which could displace an already ordered surface atom.[Deniz 2011, Barranco 2016] (see Barranco et al., Progress in Materials Science 76, 59-153 (2016)). Obliquely deposited adatoms are expected to retain part of their momentum in the direction parallel to the surface, enhancing mobility until the atom comes to rest at a local potential energy minima in the ordered $L1_0$ position.

Table I. The static and dynamic properties of FePd thin films with different buffer/seed layer combinations and oblique and normal deposition. Numbers in parentheses reflect one-sigma uncertainty from least-squares fitting of magnetization data, ferromagnetic resonance data and x-ray peak-fitting of the (002) $L1_0$ FePd reflection.

Layer Stack	M_s(kA/m)	α	$\mu_0 H_{\mathrm{eff}}^{\perp}$ (T)	K_U (MJ/m^3)	$\mu_0 H_c$ (T)	c(Å)	S
Cr/Pt (Oblique)	1000(50)	0.010(2)	0.537(2)	0.90(6)	0.030(5)	3.694(3)	0.71(2)
Cr/Pt (Normal)	950(50)	0.015(2)	0.410(1)	0.76(5)	0.025(5)	3.708(6)	0.64(4)
Cr/Ir (Oblique)	1000(50)	0.055(22)	0.40(3)	0.83(6)	0.045(5)	3.706(8)	0.68(4)
Cr/Ir (Normal)	900(50)	0.026(25)	0.24(4)	0.62(6)	0.030(5)	3.697(5)	0.58(5)
Cr/Ru (Oblique)	1000(50)	0.015(4)	0.013(9)	0.64(6)	0.015(5)	3.658(10)	0.67(5)
Cr/Ru (Normal)	850(50)	0.012(1)	-0.001(2)	0.45(5)	0.010(5)	3.642(8)	0.56(2)

4. CONCLUSION

Oblique and normal deposition was employed to address best practices for FePd growth across three prospective buffer layer materials. The $L1_0$ order parameter systematically rose with obliquely deposited FePd films compared to those in which the substrate was facing the sputtering target during FePd sputter deposition. Moreover, compared to normal deposition, the oblique deposition has a larger perpendicular magnetic anisotropy, magnetic coercive fields, and more squareness of magnetic hysteresis loops, all of which are consistent with the observed enhanced $L1_0$ ordering. Along with a relatively low Gilbert damping, oblique deposition delivered the best combination of damping (0.010) and anisotropy energy (0.90 MJ/m^3) in a Cr/Pt-buffered FePd film. While it is possible that additional post-deposition annealing could improve these magnetic properties further, along with the moderate order parameter (0.71), the ability to achieve these values under relatively low temperature deposition (350 ºC) is highly favorable for prospective semiconductor integrated magnetic memory devices.

ACKNOWLEDGMENT

This work is funded in part by Defense Advanced Research Projects Agency HR001117S0056—FP—02 "Advanced MTJs for computation in and near random access memory," and the National Institute of Standards and Technology.

REFERENCES

Ali Z, Basaula D, Zhou W, Brock J, Khan M, Eid K F (2019), "Controlling the charge transport mode in permalloy films using oblique angle deposition," *Journal of Magnetism and Magnetic Materials,* vol. 484, pp. 430-436, doi: 10.1016/j.jmmm.2019.03.087.

Alvarez R, Garcia-Martin J M, Garcia-Valenzuela A, Macias-Montero M, Ferrer F J, Santiso J, Rico V, Cotrino J, Gonzalez-Elipe A R, Palmero A (2016), "Nanostructured Ti thin films by magnetron sputtering at oblique angles," *Journal of Physics D: Applied Physics,* vol. 49, doi: 10.1088/0022-3727/49/4/045303.

Barranco A, Borras A, Gonzalez-Elipe A R, Palmero A (2016), "Perspectives on oblique angle deposition of thin films: From fundamentals to devices," *Progress in Materials Science,* vol. 76, pp. 59-153, doi: https://doi.org/10.1016/j.pmatsci.2015.06.003.

Bhatti S, Sbiaa R, Hirohata A, Ohno H, Fukami S, Piramanayagam S N (2017), "Spintronics based random access memory: a review," *Materials Today,* vol. 20, pp. 530-548, doi: https://doi.org/10.1016/j.mattod.2017.07.007.

Caro P, Cebollada A, Ravelosona D, Briones F, García D, Vázquez M, Hernando A (1997), "The influence of the Pt buffer layer on the perpendicular magnetic anisotropy in epitaxial FePd(001) ordered alloys grown by sputtering," *Journal of Applied Physics,* vol. 81, pp. 5050-5052, doi: 10.1063/1.364504.

Chang H W, Yuan F T, Chen W C, Wei D H, Lin M C, Su C C, Wang C R, Shih C W, Chang W C, Yao Y D (2015), "Hard Magnetic Property Improvement of Sputter-Prepared FePd Films on Glass Substrates by Underlayering With Refractory Nb, Mo, and W Elements," *Ieee Transactions on Magnetics,* vol. 51, 2102904, p. 4, doi: 10.1109/tmag.2015.2438896.

Deniz D, Lad R J (2011), "Temperature threshold for nanorod structuring of metal and oxide films grown by glancing angle deposition," *Journal of Vacuum Science & Technology A: Vacuum, Surfaces, and Films,* vol. 29, doi: 10.1116/1.3525882.

Farle M, Mirwald-Schulz B, Anisimov A N, Platow W, Baberschke K (1997), "Higher-order magnetic anisotropies and the nature of the spin-reorientation transition in face-centered-tetragonal Ni(001)/Cu(001)," *Physical Review B,* vol. 55, pp. 3708-3715, doi: 10.1103/PhysRevB.55.3708.

Fernández-Pacheco A, Vedmedenko E, Ummelen F, Mansell R, Petit D, Cowburn R P (2019), "Symmetry-breaking interlayer Dzyaloshinskii–Moriya interactions in synthetic antiferromagnets," *Nature Materials,* vol. 18, pp. 679-684, doi: 10.1038/s41563-019-0386-4.

Futamoto M, Nakamura M, Ohtake M, Inaba N, Shimotsu T (2016a), "Growth of L10-ordered crystal in FePt and FePd thin films on MgO(001) substrate," *AIP Advances,* vol. 6, p. 085302, doi: 10.1063/1.4960554.

Futamoto M, Nakamura M, Ohtake M, Inaba N, Shimotsu T (2016b), "Growth of L1(0)-ordered crystal in FePt and FePd thin films on MgO(001) substrate," *Aip Advances,* vol. 6, 085302, p. 11, doi: 10.1063/1.4960554.

He K H, Chen J S (2013), "First principles study of magnetic anisotropy and magnetoelectric effect of FePd/MgO(001) ultrathin films," *Journal of Applied Physics,* vol. 113, 17c702, p. 3, doi: 10.1063/1.4793601.

Hsu W H, Bell R, Victora R H (2018), "Ultra-Low Write Energy Composite Free Layer Spin-Orbit Torque MRAM," *Ieee Transactions on Magnetics,* vol. 54, 3401205, p. 5, doi: 10.1109/tmag.2018.2847235.

Ikeda S, Miura K, Yamamoto H, Mizunuma K, Gan H D, Endo M, Kanai S, Hayakawa J, Matsukura F, Ohno H (2010), "A perpendicular-anisotropy CoFeB–MgO magnetic tunnel junction," *Nature Materials,* vol. 9, pp. 721-724, doi: 10.1038/nmat2804.

Kaidatzis A, Gopman D B, Bran C, García-Martín J M, Vázquez M, Niarchos D (2019), "Investigation of split CoFeB/Ta/CoFeB/MgO stacks for magnetic memories applications," *Journal of Magnetism and Magnetic Materials,* vol. 473, pp. 355-359.

Kent A D, Worledge D C (2015), "A new spin on magnetic memories," *Nature Nanotechnology,* vol. 10, pp. 187-191, doi: 10.1038/nnano.2015.24.

Krounbi M, Nikitin V, Apalkov D, Lee J, Tang X, Beach R, Erickson D, Chen E (2015), "(Keynote) Status and Challenges in Spin-Transfer Torque MRAM Technology," *ECS Transactions,* vol. 69, pp. 119-126, doi: 10.1149/06903.0119ecst.

Lee H R, Lee K, Cho J, Choi Y H, You C Y, Jung M H, Bonell F, Shiota Y, Miwa S, Suzuki Y (2014), "Spin-orbit torque in a bulk perpendicular magnetic anisotropy Pd/FePd/MgO system," *Scientific Reports,* vol. 4, 6548, p. 7, doi: 10.1038/srep06548.

Liu T, Ma L, Zhao S Q, Ma D D, Li L, Cheng G, Rao G H (2017), "Crystal structure and magnetic properties of FexPd1-x thin films annealed at 550 A degrees C," *Journal of Materials Science-Materials in Electronics,* vol. 28, pp. 3616-3620, doi: 10.1007/s10854-016-5963-6.

Mangin S, Ravelosona D, Katine J A, Carey M J, Terris B D, Fullerton E E (2006), "Current-induced magnetization reversal in nanopillars with perpendicular anisotropy," *Nature Materials,* vol. 5, pp. 210-215, doi: 10.1038/nmat1595.

Meng H, Wang J-P (2006), "Spin transfer in nanomagnetic devices with perpendicular anisotropy," *Applied Physics Letters,* vol. 88, p. 172506, doi: 10.1063/1.2198797.

Naganuma H, Kirn G, Kawada Y, Inami N, Hatakeyama K, Iihama S, Islam K M N, Oogane M, Mizukami S, Ando Y (2015), "Electrical Detection of Millimeter-Waves by Magnetic Tunnel Junctions Using Perpendicular Magnetized L1(0)-FePd Free Layer," *Nano Letters,* vol. 15, pp. 623-628, doi: 10.1021/nl504114v.

Ohtake M, Yabuhara O, Tobari K, Kirino F, Futamoto M (2011), "Structure and magnetic properties of FePd-alloy epitaxial thin films grown on MgO single-crystal substrates with different orientations," *Journal of Applied Physics,* vol. 109, p. 07B757, doi: 10.1063/1.3563038.

Ohtake M, Itabashi A, Futamoto M, Kirino F, Inaba N (2015), "Crystal Orientation, Order Degree, and Surface Roughness of FePd-Alloy Film Formed on MgO(001) Substrate," *Ieee Transactions on Magnetics,* vol. 51, 2100904, p. 4, doi: 10.1109/tmag.2015.2434883.

Saito T, Hamashima M, Saito C, Nakamura M, Okazaki T, Furuya Y, Muro H (2013), "Cantilever-Type FePd/PZT Stacked-Layer Magnetic Sensors with High Sensitivity," *Electronics and Communications in Japan,* vol. 96, pp. 8-15, doi: 10.1002/ecj.11533.

Sun A C, Hsu J-H, Yuan F T (2010), "Control of growth and ordering process in FePt(001) film at 300 0 C," *Journal of Physics Conference Series (Online),* vol. 200, p. 4, doi: DOI:101088/1742-6596/200/10/102009.

Tokuoka Y, Seto Y, Kato T, Iwata S (2014), "Effect of Ag addition to L1(0) FePt and L1(0) FePd films grown by molecular beam epitaxy," *Journal of Applied Physics,* vol. 115, 17b716, doi: 10.1063/1.4864251.

Vrakatseli V E, Kalarakis A N, Kalampounias A G, Amanatides E K, Mataras D S (2018), "Glancing Angle Deposition Effect on Structure and Light-Induced Wettability of RF-Sputtered TiO(2) Thin Films," *Micromachines (Basel),* vol. 9, doi: 10.3390/mi9080389.

Weisheit M, Faehler S, Marty A, Souche Y, Poinsignon C, Givord D (2007), "Electric field-induced modification of magnetism in thin-film ferromagnets," *Science,* vol. 315, pp. 349-351, doi: 10.1126/science.1136629.

Xu S J, Shi Z, Zhou S M (2018), "Clear evidence of interfacial anomalous Hall effect in epitaxial L1(0) FePt and FePd films," *Physical Review B,* vol. 98, 024413, p. 5, doi: 10.1103/PhysRevB.98.024413.

Xu Y, Chen J S, Wang J P (2002), "In situ ordering of FePt thin films with face-centered-tetragonal (001) texture on Cr100−xRux underlayer at low substrate temperature," *Applied Physics Letters,* vol. 80, pp. 3325-3327, doi: 10.1063/1.1476706.

Yang E, Laughlin D E, Zhu J (2012), "Correction of Order Parameter Calculations for FePt Perpendicular Thin Films," *IEEE Transactions on Magnetics,* vol. 48, pp. 7-12.

Yang Y T, Wang D H, Song Y Q, Gao J L, Lv L Y, Cao Q Q, Du Y W (2013), "Electric-field-assisted magnetization switching in FePd/Pb(Mg1/3Nb2/3)O-3-PbTiO3 heterostructure at room temperature," *Journal of Applied Physics,* vol. 114, 144902, p. 3, doi: 10.1063/1.4824542.

Yang Y T, Song Y Q, Wang D H, Gao J L, Lv L Y, Cao Q Q, Du Y W (2014), "Electric field control of magnetism in FePd/PMN-PT heterostructure for magnetoelectric memory devices," *Journal of Applied Physics,* vol. 115, 024903, p. 3, doi: 10.1063/1.4861618.

Zhang D-L, Sun C, Lv Y, Schliep K B, Zhao Z, Chen J-Y, Voyles P M, Wang J-P (2018a), "${L1}_{0}\text{ }\mathrm{Fe}\text{\ensuremath{-}}\mathrm{Pd}$ Synthetic Antiferromagnet through an fcc Ru Spacer Utilized for Perpendicular Magnetic Tunnel Junctions," *Physical Review Applied,* vol. 9, p. 044028, doi: 10.1103/PhysRevApplied.9.044028.

Zhang D L, Schliep K B, Wu R J, Quarterman P, Hickey D R, Lv Y, Chao X H, Li H S, Chen J Y, Zhao Z Y, Jamali M, Mkhoyan K A, Wang J P (2018b), "Enhancement of tunneling magnetoresistance by inserting a diffusion barrier in L1(0)-FePd perpendicular magnetic tunnel junctions," *Applied Physics Letters,* vol. 112, 152401, p. 5, doi: 10.1063/1.5019193.

Zheng Y F, Wang J P, Ng V (2002), "Control of the tilted orientation of CoCrPt/Ti thin film media by collimated sputtering," *Journal of Applied Physics,* vol. 91, pp. 8007-8009, doi: 10.1063/1.1456416.